

Advanced Antenna Design Using Radio Frequency Liquid Crystals And LCD Manufacturing

Ryan A. Stevenson^{*a}, Mohsen Sazegar^a, Phillip Sullivan^a
^aKymeta Corporation, 12277 134th Court NE, Redmond, WA, USA 98052

ABSTRACT

For broadband, mobile satellite communications applications such as autonomous driving, a high gain, scanning antenna is required. The satellite communications industry, however, is dominated by dish antennas mounted on motorized gimbals for these use cases. These solutions are too large, heavy, and power-consuming to offer solutions for consumer applications. We have addressed these issues by commercializing a novel, electronically scanned antenna technology, which is achieved using diffractive metasurfaces and high-birefringence radio frequency liquid crystals. This technology is positioned for mass production by leveraging the manufacturing capabilities of the LC display industry.

Keywords: Metamaterials; leaky wave antennas; radio frequency liquid crystals, high birefringence liquid crystals

1. INTRODUCTION

Broadband satellite communications use cases where the platform is mobile, where the satellite is non-geostationary, or both, require a high-gain, scanning antenna. Consumer applications dictate a high-performance antenna solution that is both cheap and reliable. The mobile satellite communications industry, however, is dominated by dish antennas mounted on motorized gimbals. These solutions are too large, heavy, and power-consuming to offer solutions for consumer applications such as the connected automobile, or user terminals for next-generation Low Earth Orbit (LEO) satellite constellations. The other alternative is phased array technology. This technology is typically available only to non-consumer (e.g. enterprise, government, and military) market verticals, however, because of its expense and power consumption.

We have overcome these limitations by commercializing an electronically-scanned antenna technology, based on a diffractive metamaterials concept, called Metamaterial Surface Antenna Technology (MSAT). Electronic scanning is achieved using high-birefringence liquid crystals. The use of liquid crystals (LC) as a tunable dielectric at microwave frequencies permits large-angle ($< 30^\circ$) beam elevation scanning and fast tracking ($\sim 30^\circ/\text{sec}$), with power consumption of < 15 Watts and antenna thickness ~ 5.0 cm and no moving parts. Kymeta's engineering approach, using LC and optimization of the materials and design for compatibility with liquid crystal display (LCD) manufacturing processes, positions the technology for mass production by leveraging the capital infrastructure of the LCD industry.

The remainder of this report is outlined as follows: Section 2 provides an overview of radio frequency liquid crystal (RFLC) materials and design considerations; Section 3 presents diffractive metasurfaces and holographic beam forming; Section 4 provides discussion of results and antenna performance; Section 6 concludes.

2. RADIO FREQUENCY LIQUID CRYSTALS

RFLCs typically consist of uniaxial nematic liquid crystals; however, for practical microwave device applications the birefringence is significantly larger than conventional LC display liquid crystals. Prior work with LC-based microwave antennas has focused on producing phase shifters for phased-array antennas with improved figures of merit (FoM) over traditional microwave phase shifters¹. The requirements for RFLCs in the MSAT approach are significantly different than with LC-based phase shifters. The FoM for LC phase shifters is heavily weighted towards reduced microwave losses, rather than large birefringence². As discussed by Fritzsche, et. al., first generation microwave liquid crystals made

*ryan@kymetacorp.com; phone (425)896-3700; www.kymetacorp.com

incremental advances over traditional display liquid crystals (e.g., K15 and E7) in both tunability and loss, with two distinct development efforts to push for either lower loss or higher tunability³. MSAT requires large changes in the relative permittivity with a tunability of roughly 35%-40%. The phase shifter approach, in contrast, sees tunabilities of typically ~20%, where the tunability is defined as:

$$\tau = \frac{\epsilon_{\parallel} - \epsilon_{\perp}}{\epsilon_{\perp}} \quad (1)$$

In equation 1, ϵ_{\parallel} and ϵ_{\perp} are the parallel and perpendicular microwave permittivity corresponding to the long axis and short axes of the LC molecule, as shown in Figure 1.

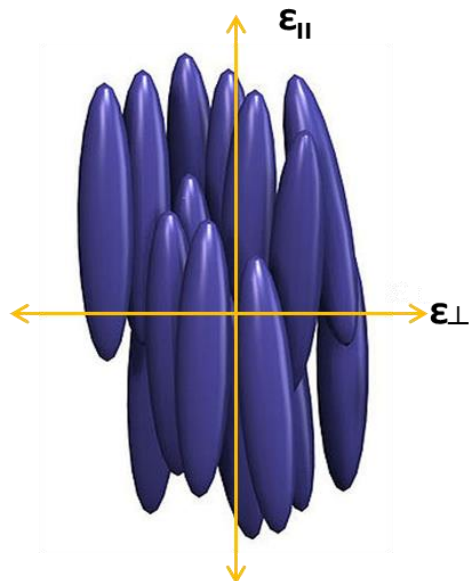


Figure 1. RFLC Geometric orientation

High birefringence LCs, hence large microwave tunabilities, are achieved through LC molecules with large electron polarizability anisotropy⁴. This effect is most prominent in molecules with long, conjugated π -electron systems. Molecules that optimize several important parameters tend to consist of rigid cores of benzene rings either directly connected or connected through an ethynyl bridge (tolane structure) as shown in Figure 2⁵.

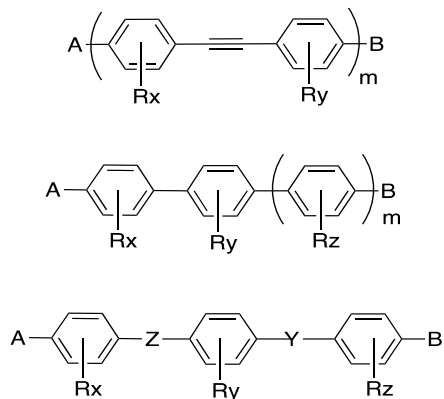


Figure 2. General chemical core structures for high birefringence LCs

In Figure 2, the top and middle core structures are expressed in terms of units of number, m . All three structures can be laterally functionalized at the R positions, most commonly with protons, H, and/or heteroatoms such as fluorine, bromine, or chlorine. Alkyl groups, e.g. methyl, ethyl, or methoxy, ethoxy, etc. may be introduced at the various R positions as well. This lateral functionalization modifies intermolecular interactions in order to discourage smectic phase formation and/or to modify rotational viscosity, elastic constants, and melting point. Lengthening the core (increasing m) increases birefringence as a general rule. Terminal functionalization has two primary considerations. First, in order to reduce the melting point and favor nematic phase formation, a long carbon tail is attached at the A position. Second, at the B position a polar end group, such as cyano (CN) or isothiocyanate (NCS) is used to further increase birefringence and introduce a permanent dipole.

3. DIFFRACTIVE METASURFACES AND HOLOGRAPHIC BEAM FORMING

Recently, three-dimensional, refractive metamaterial approaches have been extended to two-dimensional surfaces, or metasurfaces⁶. Metasurfaces have several advantages over traditional bulk metamaterials, namely that they take up less physical space and have the potential for less-lossy structures. Metasurfaces are characterized by both the periodicity of scatterers and thickness of the surface being small relative to the wavelength of interest. We are leveraging the metasurface concept, in conjunction with diffractive beamforming principles to commercialize MSAT⁷.

The MSAT approach is a leaky wave approach in which the antenna aperture is synthesized from a large number of sub-wavelength radiating elements. With MSAT (see Figure 3) each antenna element is coupled to a travelling wave feed structure comprised of a microwave waveguide. In the example shown in Figure 3, antenna elements are placed along the broad wall of a rectangular waveguide. Near their resonant frequency, the antenna elements couple energy from the feed wave and scatter this energy from the surface of the antenna. Antenna elements that have been detuned from their resonant frequency do not scatter energy from the feed wave. Due to the dense spacing of elements along the direction of the feed wave, elements with the correct phase to interfere constructively and produce radiation at the desired angle can be tuned to radiate (turned “on”). Elements with the wrong phase (otherwise resulting in destructive interference) can be detuned and prevented from radiating (turned “off”). The pattern of “on” and “off” elements, hence the antenna beam pointing angle and polarization state, can be changed dynamically in software.

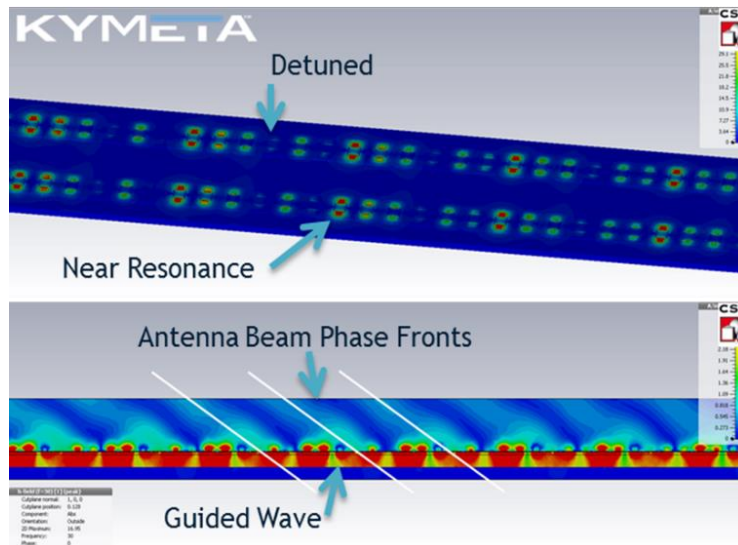


Figure 3. Top view and cross section showing the antenna elements, feed structure, and the antenna beam produced from the pattern of radiating and non-radiating elements.

The pattern of activated and deactivated antenna elements is determined from a holographic beam forming principle. With this approach, the feed wave is analogous to a reference beam (equation 1), and the wave coming off the antenna is analogous to an object beam (equation 2). Hence, the antenna surface becomes a diffractive grating, where the diffraction

pattern is determined by the interference of these two waves (equation 3):

$$\Psi_{ref} \approx \exp(-i\vec{k}_s \cdot \vec{r}) \quad (2)$$

$$\Psi_{obj} = \exp(-i\vec{k}_f(\theta_o, \phi_o) \cdot \vec{r}) \quad (3)$$

$$\Psi_{intf} = \Psi_{obj}\Psi_{ref}^* \quad (4)$$

In the equations above, \vec{k}_s is the feed wave wavenumber, \vec{k}_f is the free space wavenumber, which is a function of the desired azimuth and elevation scan angles, and * denotes the complex conjugate. This calculation is run onboard the antenna control electronics so that as the look angle between the antenna and the satellite changes, azimuth and elevation are updated and a new diffraction pattern to produce the beam at the new look angle is generated. The amplitude of scattered energy from each individual radiating element on the surface of the array is then controlled to reproduce this diffraction pattern.

A key differentiator between MSAT and other resonant metamaterial phenomena is that the diffraction pattern on the metasurface is produced through tuning of element resonances, but the antenna beam is not produced on a resonance. Thus, the antenna bandwidth is not limited by the resonance of the elements themselves (a typical problem with resonant metamaterials) but by the tunability of the elements. MSAT, therefore, can achieve broadband operation as required for high-throughput satellite communications.

As discussed previously, the resonant frequency of each antenna element is adjusted to change the amount of microwave energy scattered from those elements. Referring to the circuit model shown in Figure 4, there is a portion of the capacitance of each element that is tunable, producing a resonant frequency shift as $1/\sqrt{L \cdot C}$, where L is the inductance of the antenna element and C is the capacitance. The capacitance of the antenna element is adjusted by using the LC as a tunable dielectric constant and varying the voltage across the LC cell.

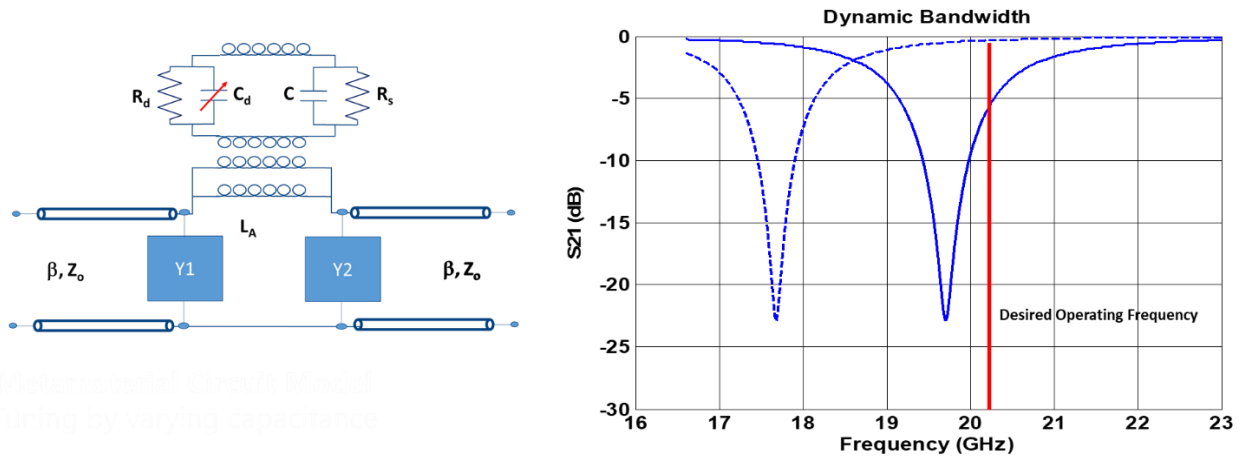


Figure 4. Transmission line model of an MSAT antenna element coupled to the feed line and resultant insertion loss for the tuned and detuned states

The plot in Figure 4 shows the insertion loss of the two-port transmission line model for an antenna element inductively coupled to the transmission line in both the tuned and detuned states. In this example the desired operating frequency is around 20 GHz. For an antenna element near resonance (solid line), the low insertion loss indicates that energy is being

radiated by the antenna element. For the detuned element (dashed line), the insertion loss is near zero, indicating that little energy is being radiated.

The amplitude contrast between tuned and detuned states at the operating frequency demonstrates how an amplitude hologram can be formed in the metasurface. Considering the tunability discussion presented in section 2, higher birefringence LCs can attain more frequency separation between tuned and detuned states, hence more amplitude contrast ratio and more dynamic bandwidth.

4. MANUFACTURING RESULTS AND ANTENNA PERFORMANCE

The metasurface construction, with an upper and lower substrate/electrode and LC as the tunable medium, closely resembles the assembly of an LC display. Array elements are individually addressed in an active matrix addressing scheme using printed thin film transistors (TFT), exactly as typical displays are made. The metasurface for our Ku-band product is currently produced on commercial LCD manufacturing lines. Figure 5 shows an antenna segment on a manufacturing line and the resultant antenna aperture assembly.

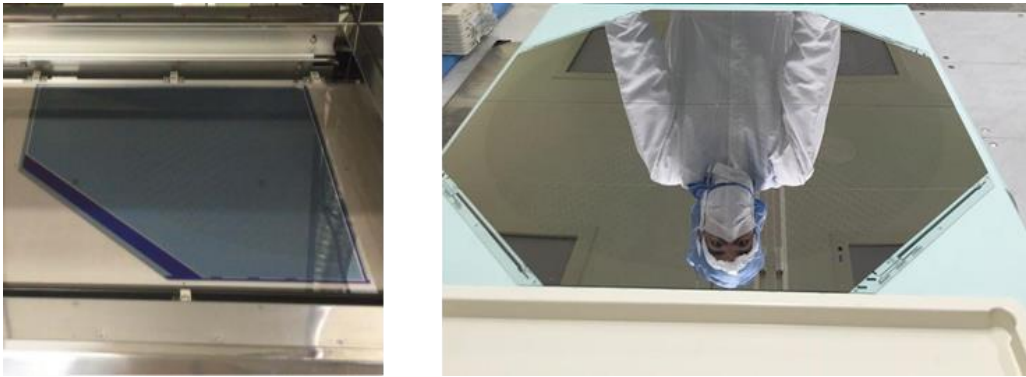


Figure 5. An antenna segment in production and the complete 70 cm Ku-band antenna aperture assembly

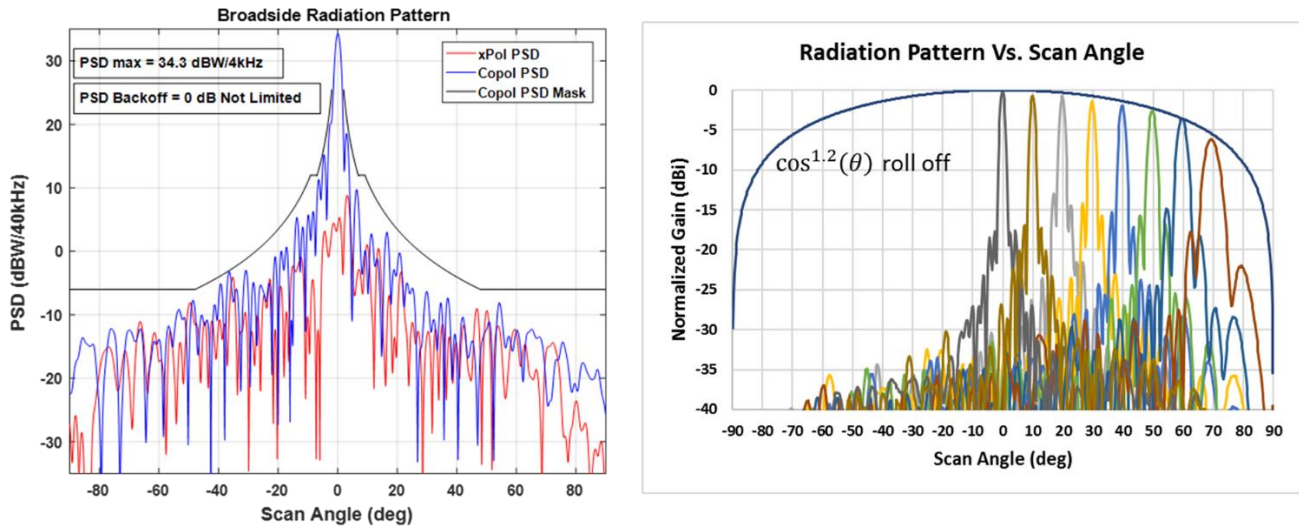


Figure 6. Co-polarized and cross-polarized broadside beam patterns shown against the ITU power spectral density mask and radiation pattern as a function of scan angle for the Kymeta 70 cm Ku-band antenna.

MSAT trades off discrete amplitude and phase control of each antenna element (phased array), for the manufacturability and cost of the diffractive metasurface approach. While dramatically lowering cost and power consumption over phased

array and achieving consumer electronics scale manufacturing, MSAT has also demonstrated noteworthy technical capabilities for a flat-panel, electronically scanned antenna:

- Full duplex receive/transmit from a single physical aperture
- Dynamically adjustable polarization from tracking linear to circular (RHCP and LHCP)
- Full 360° azimuth scanning and elevation scanning below 15° with return loss independent of scan angle
- Compliance with ITU and FCC power spectral density (PSD) masks

Figure 6 shows a broadside beam pattern for our Ku-band 70 cm antenna at 14.25 GHz, where compliance against the ITU mask is shown without power back-off. Broadside performance achieves a dynamic bandwidth of 1 GHz on receive (11.4-12.4 GHz), instantaneous bandwidth > 100 MHz, and peak G/T of 9.5 dB/K. Excellent scan loss results are achieved through the use of a passive wide angle impedance matching (WAIM) metasurface structure. Without this feature the scan loss would follow $\cos^2(\theta)$, which would yield 6 dB scan loss at 60-degree scan angle.

5. CONCLUSION

With MSAT we have addressed the key technical challenges associated with 3D, resonant metamaterials and have demonstrated high-gain, electronically scanned arrays in both the Ku and Ka satellite bands. The size, weight, power, performance and manufacturing of MSAT make it well positioned to address high-volume, low-cost mobile satellite opportunities.



Figure 7. The 70 cm Ku-band antenna product mounted flush in the roof of a test vehicle

REFERENCES

- [1] O. H. Karabey, *et al.*, “Methods for Improving the Tuning Efficiency of Liquid Crystal Based Tunable Phase Shifters,” Proc. 6th European Microwave Integrated Circuits Conference (EuMA 2011), pp. 494-497 (2011)
- [2] S. Mueller, *et al.*, “Broad-Band Microwave Characterization of Liquid Crystals Using a Temperature-Controlled Coaxial Transmission Line,” IEEE Trans. Microwave Theory Tech, vol. 53, no. 6, pp. 1937-1945 (2005)
- [3] Fritzsche, C., Wittek, M., “Recent Developments in Liquid Crystals for Microwave Applications,” 2017 IEEE Sym. Ant. Prop. (APS-2017), pp. 1217-1218 (2017)
- [4] Dabrowski, R., Przemyslaw, K., and Herman, J., “High Birefringence Liquid Crystals,” Crystals, Vol. 3, pp. 443-

482 (2013)

- [5] Sullivan, Philip A., et. al., "Radio Frequency Liquid Crystal (RFLC) Mixtures With High RF Tuning, Broad Thermal Operating Ranges, and Low Viscosity," US Patent No. 10,224,620
- [6] C.L. Holloway, E.F. Keuster, J.A. Gordon, J. O'hara, J. Booth, and D.R. Smith, "An Overview of the Theory and Applications of Metasurfaces: The Two-Dimensional Equivalents of Metamaterials," IEEE Ant. Prop. Mag., Vol. 54, No. 2, pp. 10-35 (2012)
- [7] K.M. Palmer, "Intellectual Ventures Invents Beam-Steering Metamaterials Antenna," IEEE Spectrum, November 30th (2011)